Optimal heterogeneity of a highly renewable pan-European electricity system

Emil H. Eriksen[a], Martin Greiner[b]

[a]*Department of Physics and Astronomy, Aarhus University, 8000 Aarhus C, Denmark*
[b]*Department of Engineering, Aarhus University, 8200 Aarhus, Denmark*

Abstract

The resource quality and the temporal generation pattern of variable renewable energy sources vary significantly across Europe. A homogeneous spatial distribution of wind and solar capacities makes inefficient use of the resources, resulting in high system costs. A heterogeneous spatial distribution of renewable assets maximising the overall capacity factor results in smaller investments in renewable capacities, but higher costs of transmission. A local search routine is used to find optimal distributions of generation capacities minimising backup, transmission and renewable capacity costs simultaneously, resulting in lower costs of electricity.

Keywords: renewable energy system, levelised cost of electricity, wind power generation, solar power generation

1. Introduction

The ambitious renewable targets set by the European leaders [1] imply that the renewable penetration will increase significantly in the years to come. Electrification of transportation and other sectors will play a major role in the transition [2, 3]. At present, the leading renewable technologies are wind, solar PV and hydro, of which only wind and solar PV have potential for large scale expansion. For this reason, only wind and solar PV are modelled explicitly. Since wind and solar PV are both variable renewable energy resources (VRES), backup generation is needed if power outages are to be avoided. Backup generation introduce additional system costs and must thus be kept at a minimum.

The backup requirements depend on the mismatch between VRES generation and load. Using the degrees of freedom associated with the choice of VRES assignments, it is possible to smooth out the aggregated temporal generation pattern or even shape it towards the load pattern. As a result, the mismatch (and thus the backup requirements) is lowered. To decrease the dimensionality of the problem, the renewable assets are often assigned proportional to the mean load of a country in accordance with a homogeneous wind/solar mixing factor. This approach is demonstrated in [4, 5] where balancing and storage optimal wind/solar mixes are found.

Further reductions in backup requirements are possible by exchanging energy between the countries through a transmission network [6, 7]. Other relevant papers on the advantages and costs of grid extensions are [8, 9].

In a conventional energy system, the siting of generation capacities is not a concern. No geographical areas are preferable, so the power plants are simply put where the demand is present. For VRES, the situation is more complicated. The primary reason is the geographical variation of the VRES quality. The resource quality is quantified through the capacity factor defined as

$$\mathrm{CF} = \frac{\text{Average generation}}{\text{Rated capacity}}. \tag{1}$$

The capacity factor is a number between 0 and 1, where 0 means no generation and 1 means maximum generation at all times. Capacity factors for the European countries for onshore wind, offshore wind and solar PV are listed in table 1. The capacity factors were calculated using the Renewable Energy Atlas [10] (REA). The VRES layout at country level was chosen as a homogeneous distribution across the 50% best sites. For wind conversion, a multi turbine corrected power curve for the Vestas V90 3.0 MW turbine at 80 meter hub height was assumed. For solar conversion, the Solar First Series 4 PV panel oriented south and tiled from horizontal to a degree equal to the latitude of installation was applied.

The second reason is the geographical variation of the temporal generation pattern for a given VRES type. This effect is particularly important for wind since Europe is large compared to the correlation length of wind [11]. Similar to the optimal wind/solar mixes found in [4, 5], optimal layouts of each VRES in terms of e.g. balancing can be derived.

With these points in mind, allocating resources proportional to the mean load of a country in accordance with a homogeneous wind/solar mixing factor does not seem ideal. In this paper, the effect of lifting this homogeneous assumption is explored. Different approaches to cope with the resulting large number of degrees of freedom are considered ranging from heuristic layouts constructed from

Email addresses: emilhe@phys.au.dk (Emil H. Eriksen), greiner@eng.au.dk (Martin Greiner)

Table 1: Capacity factors CF_n^w, $\mathrm{CF}_n^{\tilde{w}}$ and CF_n^s for onshore wind, offshore wind and solar PV for the European countries.

	$\mathbf{CF}_n^w$	$\mathbf{CF}_n^{\tilde{w}}$	$\mathbf{CF}_n^s$		$\mathbf{CF}_n^w$	$\mathbf{CF}_n^{\tilde{w}}$	$\mathbf{CF}_n^s$		$\mathbf{CF}_n^w$	$\mathbf{CF}_n^{\tilde{w}}$	$\mathbf{CF}_n^s$
AT	0.13	-	0.16	DE	0.20	0.44	0.14	NO	0.25	0.36	0.13
BE	0.22	0.40	0.14	GB	0.32	0.44	0.13	PL	0.17	0.34	0.14
BA	0.13	-	0.18	GR	0.14	0.34	0.19	PT	0.18	0.20	0.20
BG	0.12	0.19	0.18	HU	0.12	-	0.17	RO	0.11	0.24	0.18
HR	0.17	0.23	0.18	IE	0.35	0.38	0.11	RS	0.09	-	0.18
CZ	0.15	-	0.16	IT	0.13	0.17	0.19	SK	0.12	-	0.16
DK	0.37	0.45	0.13	LV	0.23	0.34	0.13	SI	0.07	-	0.16
EE	0.26	0.32	0.13	LT	0.20	0.32	0.13	ES	0.15	0.21	0.20
FI	0.18	0.33	0.11	LU	0.19	-	0.14	SE	0.21	0.32	0.13
FR	0.20	0.34	0.17	NL	0.27	0.43	0.13	CH	0.13	-	0.18

resource quality knowledge to layouts obtained through numerical optimization. The objective is to find heterogeneous spatial layouts with properties superior to the homogeneous layouts, in particular a lower cost of electricity. This paper is organised as follows: Section 2 discusses the general modelling of the electricity system, the key metrics and the construction of heterogeneous layouts. In section 3 the performance of the different layouts and the resulting renewable penetrations for individual European countries are discussed. Section 4 contains an analysis of the sensitivity of the results to reductions in solar costs and to expansions in offshore wind capacities. We conclude the paper with a discussion on the results and an outlook on future research.

2. Methods

2.1. The electricity network

The European electricity network is modelled using a simplified 30-node model, where each node represents a country. The nodal load is determined from historical data, while wind and solar generation data are calculated using a combination of weather data and physical models [10]. Initially, wind is assumed to be onshore only. For each node n the generation from VRES,

$$G_n^R(t) = G_n^W(t) + G_n^S(t), \tag{2}$$

can be expressed through two parameters. The penetration γ determines the amount of energy generated relative to the mean load of the node,

$$\langle G_n^R \rangle = \gamma_n \langle L_n \rangle, \tag{3}$$

while the mixing parameter α fixes the ratio between wind and solar,

$$\langle G_n^W \rangle = \alpha_n \langle G_n^R \rangle, \tag{4}$$

$$\langle G_n^S \rangle = (1-\alpha_n) \langle G_n^R \rangle. \tag{5}$$

The nodal difference between VRES generation and load

$$\Delta_n(t) = G_n^R(t) - L_n(t) \tag{6}$$

is called the mismatch. To avoid power outages, the demand must be met at all times. Since storage is not considered, any power deficits must be covered by backup generation. Dispatchable resources are not modelled explicitly, but are considered a part of the backup generation. If $\Delta_n(t) \geq 0$, excess energy must be curtailed $C_n(t)$, while if $\Delta_n(t) < 0$ backup generation $G_n^B(t)$ is needed. Together the two terms form the nodal balancing $B_n(t) = C_n(t) - G_n^B(t)$. It is possible to lower the balancing needs by transmission. Nodes with excess generation export energy $E_n(t)$, allowing nodes with an energy deficit to import energy $I_n(t)$ to (partly) cover their energy deficit. The nodal injection, $E_n(t) - I_n(t)$, is denoted $P_n(t)$. This leads to the nodal balancing equation,

$$G_n^R(t) - L_n(t) = B_n(t) + P_n(t), \tag{7}$$

The vector of nodal injections $\mathbf{P}$ is called the injection pattern. The actual imports and exports, and thus the injection pattern, depend on the business rules of the nodal interactions. It is convenient to express business rules in terms of a two step optimization problem. The top priority is to minimize the backup generation,

$$\begin{aligned} \text{Step 1:} \quad & \min_{\mathbf{P},\mathbf{F}} \quad \sum_n \frac{\left(G_n^B(t)\right)^2}{\langle L_n \rangle} \\ & \text{s.t.} \quad \sum_n P_n(t) = 0 \\ & \text{s.t.} \quad F_l^- \leq F_l(t) \leq F_l^+ \end{aligned} \tag{8}$$

where F_l is the flow on link l and $F_l^{\pm}$ denote flow constraints. By minimising B_n^2 (divided by $\langle L_n \rangle$) rather than G_n^B, the particular solution where all nodes are curtailing/generating backup synchronously (relative to $\langle L_n \rangle$) is obtained [12]. To ensure that the resulting flow resembles a physical flow, the objective is chosen as minimization of the sum of squared flows [13].

$$\text{Step 2:} \quad \begin{aligned} \min_{\mathbf{F}} \quad & \sum_l F_l(t)^2 \\ \text{s.t.} \quad & \mathbf{P}(t) = \mathbf{P}^*(t) \\ \text{s.t.} \quad & F_l^- \leq F_l(t) \leq F_l^+ \end{aligned} \tag{9}$$

where $\mathbf{P}^*$ is the injection pattern found in step 1.

2.2. Key metrics

Inspired by [14], the energy system cost is calculated based on a few key parameters. Besides the cost of the VRES capacities, $\mathcal{K}^{\mathcal{W}}$ and $\mathcal{K}^{\mathcal{S}}$, costs for the backup system and the transmission network are included. The backup system cost is split into two components, the cost of backup capacity $\mathcal{K}^B$ and the cost of backup energy E^B. The backup capacity cost covers expenses related to construction and to keeping the power plants online while the backup energy cost accounts for actual fuel costs. Expressed in units of the average annual load, the backup energy is given by

$$E^B = \frac{\sum_n \sum_t G_n^B(t)}{\sum_m \sum_t L_m(t)} = \sum_n \frac{\langle G_n^B \rangle}{\langle L_n \rangle}. \tag{10}$$

In principle, the backup capacity is fixed by a single extreme event. However with this definition, the results will be highly coupled to the particular data set used. To decrease the coupling, the 99% quantile is used rather than the maximum value,

$$q_n = \int_0^{K_n^B} p_n(G_n^B) dG_n^B, \tag{11}$$

where $p_n(G_n^B)$ is the time sampled distribution of backup generation and $q_n = 0.99$. With this choice, the backup system will be able to cover the demand 99% of the time. The remaining 1% is assumed to be covered by unmodelled balancing initiatives, e.g. demand side management. Given the nodal values $\mathcal{K}_n^B$, the overall backup capacity

$$\mathcal{K}^B = \sum_n \mathcal{K}_n^B \tag{12}$$

is calculated by summation. In analogy, the transmission capacity $\mathcal{K}_l^T$ is defined so that the flow is met 99% of the time. Transmission can be positive and negative, but since links are assumed bidirectional, only the magnitude (not the sign) of the flow is to be considered. Hence

$$q_l = \int_0^{K_l^T} p_l(|F_l|) dF_l, \tag{13}$$

where $p_l(|F_l|)$ is the time sampled distribution of absolute flows and $q_l = 0.99$. Since the link length varies, $\mathcal{K}^T$ is not calculated directly by summation, but instead as a weighted sum,

$$\mathcal{K}^T = \sum_l \mathcal{K}_l^T d_l, \tag{14}$$

where d_l denotes the length of link l. For simplicity, the link lengths are taken as the distance between neighbouring country capitals.

2.3. Cost modelling

Cost assumptions for the elements of an electricity system vary greatly across the literature [14]. In this study, the cost assumptions published by [15] have been adapted with a single modification. The cost of solar has been reduced by 50% in accordance with near future solar PV panel price projections [16]. The resulting estimates are listed in table 2. In general, the cost assumptions are in the low end for VRES which reflects the expectation that the cost of VRES will go down in the future as the penetration increases [17].

Table 2: Cost assumptions for different assets separated into capital expenditures (CapEx) and fixed/variable operational expenditures (OpEx).

Asset	**CapEx** [€/W]	**OpEx$_{\text{fixed}}$** [€/kW/y]	**OpEx$_{\text{variable}}$** [€/MWh]
CCGT	0.90	4.5	56.0
Solar PV	0.75	8.5	0.0
Offshore wind	2.00	55.0	0.0
Onshore wind	1.00	15.0	0.0

From the VRES penetration, the mixing factor and the mean load, the effective generation of each node can be calculated. Dividing by the associated capacity factor, the capacity is obtained. Except for transmission capacity, the present value of each element can be calculated directly as

$$V = \text{CapEx} + \sum_t \frac{\text{OpEx}_t}{(1+r)^t} \tag{15}$$

where r is the return rate assumed to be 4%. The transmission capacity cannot be translated directly into cost as the cost depends on the length and the type of the link. Link lengths have been estimated as the distance between the country capitals. Link costs are assumed to be 400€ per km for AC links and 1,500€ per km for HVDC links. For HVDC links, an additional cost of 150,000€ per converter station (one in each end) is added [8, 9, 18]. The layout of AC and DC links has been constructed by [6] from ENTSO-E data, se e.g. figure 1 in [14].

To allow for comparison of different energy systems, the levelised cost of electricity (LCOE) is a convenient measure. The LCOE is the cost that every unit of energy produced during the lifetime of the project must have to match the present value of investment [19],

$$\text{LCOE} = \frac{V}{\sum_t \frac{L_{EU,t}}{(1+r)^t}}. \tag{16}$$

Since the life time of the system elements differs, the LCOE is evaluated separately for each system element. The LCOE

for the complete system is calculation by summation. Life times of 25 years for solar PV and onshore wind, 20 years for offshore wind, 30 years for CCGT plants and 40 years for transmission infrastructure were assumed. See [14] for more details on the cost calculation.
Because extreme events in terms of backup capacity (all countries have a large energy deficit) and transmission capacity (some countries have an energy deficit while others have excess generation) are generally not overlapping, scaling down $\mathcal{K}^T$ with some fraction β tends to lower the LCOE since $\mathcal{K}^B$ is not increased accordingly. This point is illustrated in figure 1. The benefits of transmission have previously been studied by [20].

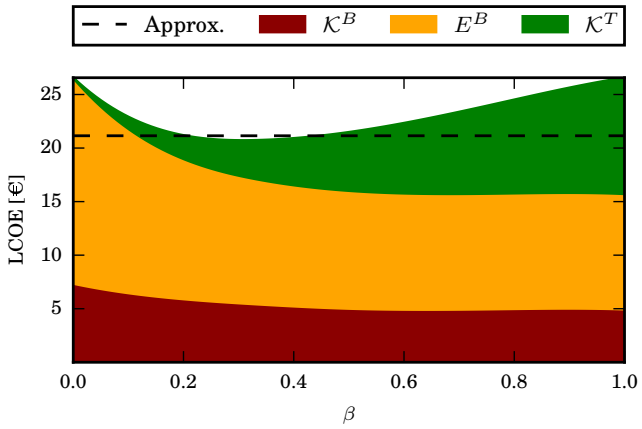

Figure 1: Non VRES LCOE components for different values of β. The dashed line indicates the approximated LCOE (see text).

Figure 1 reveals that the LCOE values at $\beta = 1$ and $\beta = 0$ are practically equal. However, in the intermediate region a significant drop in the LCOE is observed. The optimal value of β depends of the electricity system being analysed and on the specific LCOE definition (in the present case the optimum is around $\beta = \frac{1}{3}$). Obtaining the lowest possible LCOE would thus require system individual optimization. To avoid the additional complexity associated with such an optimization and to define the LCOE function in a consistent way, the LCOE will consistently be calculated using the synchronised export scheme at $\beta = 1$, but with only 50% of the $\mathcal{K}^T$ cost. The approximation is shown as a dashed line in figure 1. While the approximation is not perfect, the inaccuracy associated with the approximation is negligible compared to the uncertainty of the cost estimates.

2.4. Heuristic layouts

The simplest way to distribute the renewable resources would be to assign the resources homogeneously (relative to the mean load of the node) so that $\gamma_n = \gamma$ (and $\alpha_n = \alpha$). However this assignment might not be ideal since the capacity factors vary significantly between the nodes. Having this point in mind, an intuitive way to proceed would be to assign resources proportional to the CF. To generalise the idea, the CF is raised to an exponent β [15]. For a wind only layout, the nodal γ values are given by

$$\gamma_n^W = \gamma_{EU} \left(\mathrm{CF}_n^W\right)^\beta \frac{\langle L_{EU}\rangle}{\sum_m \langle L_m\rangle \left(\mathrm{CF}_m^W\right)^\beta} \tag{17}$$

where γ_{EU} is the overall penetration assumed to be 1. An equivalent expression for the solar only layout is obtained by the substitution $W \to S$. Examples for $\beta = 1$ are shown in figure 2. In the layout illustrations, each bar represents a country n. The height of the bar is γ_n while the mix α_n between onshore wind (blue) and solar (yellow) is expressed through the bar colouring. β layouts for any value of α can be constructed as a linear combination of the wind and solar only layouts with

$$\gamma_n = \alpha_{EU}\gamma_n^W + (1-\alpha_{EU})\gamma_n^S \tag{18}$$

and

$$\alpha_n = \frac{\alpha_{EU}\gamma_n^W}{\alpha_{EU}\gamma_n^W + (1-\alpha_{EU})\gamma_n^S}. \tag{19}$$

For practical reasons, it is not possible to realise extremely heterogeneous layouts. To constrain heterogeneity, the heterogeneity factor K is introduced by requiring

$$\frac{1}{\mathrm{K}} \leq \gamma_n \leq \mathrm{K}. \tag{20}$$

With this definition, $\mathrm{K} = 1$ corresponds to a homogeneous layout while $\mathrm{K} = \infty$ represents unconstrained heterogeneity.
Although the capacity factor of a β layout is higher than the capacity factor of the homogeneous layout (for $\beta > 0$), it is possible to achieve an even higher capacity factor without violating the constraints in equation (20). In the wind/solar PV only cases, the capacity factor is maximised by assigning $\gamma_n = \mathrm{K}$ to the countries with the highest capacity factor for wind/solar PV and $\gamma_n = \frac{1}{\mathrm{K}}$ to the remaining countries, except for a single in-between country which is fixed by the constraint

$$\sum_n \gamma_n \langle L_n\rangle = \langle L_{EU}\rangle. \tag{21}$$

Examples for $\mathrm{K} = 2$ are shown in figure 2. Similar to the β layouts, CF layouts for arbitrary α values can be constructed as linear combinations of the wind and solar PV only layouts.

2.5. Optimized layouts

The optimization objective is minimization of the LCOE with respect to the 60 variables $\gamma_1, ..., \gamma_N, \alpha_1, ..., \alpha_N$. A number of optimization algorithms were tested including the Nelder-Mead method [21], simulated annealing [22], genetic algorithms [23] and cuckoo search [24]. However, a custom local search algorithm implementation denoted Greedy Axial Search (GAS), described in Appendix I, was

found to be most effective [25]. All optimized layouts have been obtained using the GAS routine. These layouts will be denoted GAS layouts. To decrease computation time, optimisations were performed using a one year slice of the 32 year data set.

3. Results

An overview of the key parameters is shown in figure 3. For backup energy and backup capacity, the optimal mix is around $\alpha = 0.9$, which is slightly higher than the values found by [4, 5]. The difference can be attributed to differences between the REA data used in this paper and the ISET data [26] used by [4, 5]. For transmission capacity, the curves are quite similar for the β layouts with a minimum around $\alpha = 0.5$. For the CF layouts a larger increase in $\mathcal{K}^T$ is observed as K is increased. This observation is in qualitative agreement with intuition since the CF layouts are generally more extreme than the β layouts (see e.g. figure 5).
The main parameter of interest, the LCOE, has a maximum at $\alpha = 0$. It drops steadily as α is increased until around $\alpha = 0.8$ where the minimum is located. The high cost at $\alpha = 0$ is caused by a combination of high backup energy/capacity costs and the fact that the CF of solar is generally lower than for onshore wind. The cost of producing one unit of energy is thus higher for solar than for onshore wind even though the CapEx is lower for solar.
The component wise costs for the optimal β, CF and GAS layouts are shown in figure 4. From this figure it is clear that the VRES cost is dominating. Compared to the β and CF layouts, the GAS layouts include a slightly larger solar component. The magnitude of the solar component for the GAS layouts drops with increasing K value. As the heterogeneity constraints are loosened wind becomes more favourable since it becomes possible to allocate more resources to the sites with a very high CF. A similar effect is present for solar, but it is less dominant since the best CF for solar (0.20, Spain) is much smaller than for wind (0.37, Denmark).
The optimal β, CF and GAS layouts are shown in figure 5. Note that for $K = 1$, the β and the CF layouts are both equal to the homogeneous layout. From figures 5b and 5c we see that the CF and the GAS layouts are quite similar. These figures also explain why the GAS routine is able to include a solar component at a competitive cost; unlike the β and CF layout definitions, the GAS routine has the freedom to assign solar only to countries with poor wind resources, e.g. Serbia (RS) and Slovenia (SI).

4. Sensitivity analysis

4.1. Reduced solar cost

For the β as well as the CF layouts, the optimal α values are 0.84. As mentioned previously, wind domination

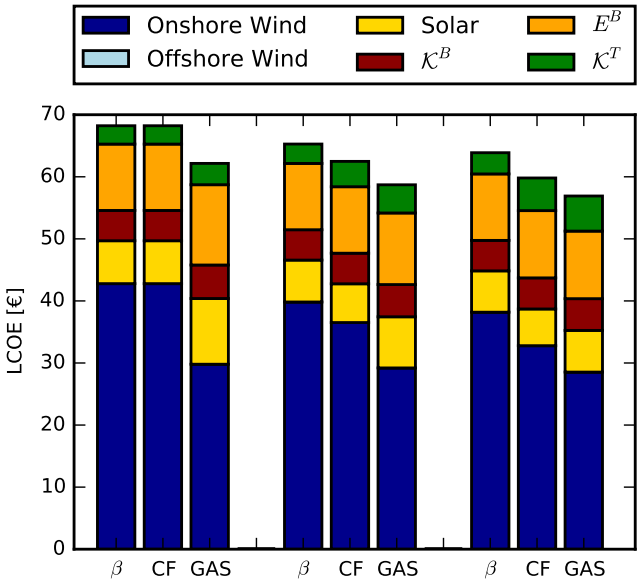

Figure 4: Component wise LCOE for the optimal β, CF and GAS layouts for K = 1 (left), 2 (middle) and 3 (right).

is partly a consequence of the higher cost of energy generation for solar PV compared to onshore wind. The cost of solar has dropped rapidly in the recent years and this tendency might very well continue. To shed some light on the consequences of further price reductions, the sensitivity of the optimal mix to reductions in the solar cost is examined. In figure 6, the LCOE as a function of α is shown (similar to the lower right of figure 3) when the solar cost is reduced by 25%, 50% and 75% respectively. The 0% scenario is included as a reference.
A reduction of the solar cost by 25% does not change the picture much. The optimal mix is shifted from above 0.8 to below 0.8 and the cost drops by around 2€ (cost comparison numbers are calculated for the GAS layouts at K = 2). As the solar cost is reduced by 50% the cost of pure solar ($\alpha = 0$) becomes comparable to the cost of pure wind ($\alpha = 1$). The optimal mix drops to around 0.6 and the LCOE is reduced by more than 5€ compared to the reference scenario. Reducing the cost of solar by 75% changes the curve shapes completely as solar is now much cheaper than wind. With values in the 0.2 to 0.6 range, the optimal mix now depends strongly on the choice of layout strategy. A cost reduction of more than 10€ is observed and for the GAS optimized layout at K = 3 the LCOE drops below the 50€ barrier.

4.2. Offshore wind

So far, wind has been assumed to be onshore only. By January 2014, the total European onshore wind capacity was 120.8GW, while the offshore capacity was 8.0GW [27]. The increasing share of offshore wind raises the question, how the LCOE will be affected by the introduction of an offshore component. The immediate expectation would

be a significant increase in the LCOE since the expenditures for offshore wind are more than 100% higher than for onshore wind due to foundation expenses and increased maintenance costs. On the other hand the capacity factors for offshore sites are generally higher than for onshore sites - but nowhere near 100%.
It would be possible to introduce offshore wind on equal footing with onshore wind and solar PV. However, since offshore wind is much more expensive, an optimized layout would pose a 0% offshore component, which is not an interesting nor surprising result. Instead, a fixed offshore component is introduced by splitting the wind component into an onshore γ^W and an offshore $\gamma^{\tilde{W}}$ component,

$$\gamma^W \rightarrow \gamma^{\mathrm{W}} + \gamma^{\tilde{W}}, \tag{22}$$

for countries with suitable offshore regions. Explicitly these are the North Sea Countries (Denmark, Germany, Great Britain, Ireland, the Netherlands, France, Belgium, Norway and Sweden). Other countries retain onshore wind only. The magnitude of the offshore component is defined by requiring that the offshore wind power generation accounts for a fixed share of the total wind power generation. Cost details for optimized layouts with fixed offshore shares of 25% and 50% are shown in figure 7. The 0% scenario is included as a reference.

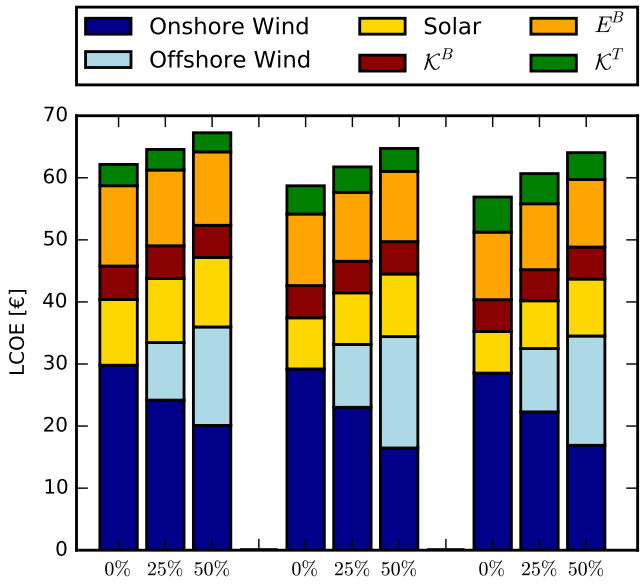

Figure 7: Cost details for the GAS optimal layouts for K = 1 (left), 2 (middle) and 3 (right) for offshore shares of 0%, 25% and 50%.

From figure 7 it is clear that the introduction of an offshore component increases the LCOE. However, the increase in LCOE is not dramatic. While the cost of wind increases significantly, the cost of backup and transmission decreases slightly. The decrease is a consequence of the difference in the temporal generation pattern from onshore to offshore wind. In some time steps the onshore generation is low while the offshore generation is high. The introduction of an offshore component thus tends to smooth out the wind generation time series. The GAS optimized layouts for an offshore share of 50% are shown in figure 8.

5. Discussion and conclusions

The dependence on the country wise layout of VRES of a number of key parameters along with the resulting LCOE has been investigated. It was found that the backup and transmission costs are significant, but the main costs are associated with the VRES capacities. The VRES capacity costs can be lowered by allocating more resources to countries with high capacity factors. At a heterogeneity factor of $K = 2$, meaning that each country installs VRES capacities covering a minimum of 50% and maximum of 200% of their mean load, the LCOE can be lowered by more than 8% by choosing the heuristic CF layout which maximises the overall capacity factor. Further reduction of the cost can be achieved by optimization. Using a local search routine such a layout was found to reduce the LCOE by an additional 5%. While the additional cost reduction of 5% is obtained by fine tuning, the primary cost reduction is of a more general nature. It can be attributed to the general tendency for the heterogeneous layouts to shift wind capacities towards the North Sea countries. Since the wind resource quality is better than for the central and southern countries, this reallocation results in lower costs.
In the past onshore wind has been the predominant VRES. However, the cost of solar PV has dropped rapidly in recent years, and solar PV has already reached grid parity in some markets [28]. If the decreasing price tendency continues much longer, the cost optimal mix might very well end up around $\alpha = 0.6$ indicating almost equal amounts of wind and solar PV installations.
The main analysis considered onshore wind only, but the effect of introducing an offshore component was also discussed. Foundation expenses and increased maintenance costs makes offshore wind significantly more expensive than onshore wind. Some of the additional expenses are compensated by higher offshore capacity factors along with a more stable temporal generation pattern, but at the end of the day, offshore wind is still more expensive than onshore wind. However, there are other incentives for offshore wind. The opposition from residents is usually lower than for onshore wind, and the potential for expansion larger. The number of suitable onshore sites are limited, and when they are exhausted, offshore wind might pose the best alternative.
In conclusion, it was found that an optimised heterogeneous layout with wind resources shifted towards the North Sea countries decreases the LCOE by around 8% compared to the homogeneous layout at the optimal mix. An additional reduction of 5% was possible by explicit optimization.

The effect of integrating one or more storage elements in the electricity system has not been considered in this pa-

per. Promising storage projects are already in the making, so by the time Europe reaches $\gamma = 1$, commercial large scale storage systems are presumably available. A natural extension of this paper would be to include various types of storage.

Bibliography

[1] European Commission. A roadmap for moving to a competitive low carbon economy in 2050. Technical report, EC, March 2011.

[2] James H. Williams, Andrew DeBenedictis, Rebecca Ghanadan, Amber Mahone, Jack Moore, William R. Morrow, Snuller Price, and Margaret S. Torn. The Technology Path to Deep Greenhouse Gas Emissions Cuts by 2050: The Pivotal Role of Electricity. Science, 335:53–59, 2012. http://dx.doi.org/10.1126/science.1208365.

[3] McKinsey & Company, KEMA, The Energy Futures Lab at Imperial College London, Oxford Economics, and ECF. Roadmap 2050 – A practical guide to a prosperous, low-carbon Europe. Technical report, European Climate Foundation, http://www.roadmap2050.eu/, April 2010. Online, accessed June 2012.

[4] Heide, D., von Bremen, L., Greiner, M., Hoffmann, C., Speckmann, M., and Bofinger, S. Seasonal optimal mix of wind and solar power in a future, highly renewable Europe. Renewable Energy, 35(11):2483–2489, 2010.

[5] Heide, D., Greiner, M., Von Bremen, L., and Hoffmann, C. Reduced storage and balancing needs in a fully renewable European power system with excess wind and solar power generation. Renewable Energy, 36(9):2515–2523, 2011.

[6] Rolando A. Rodriguez, Sarah Becker, Gorm Bruun Andresen, Dominik Heide, and Martin Greiner. Transmission needs across a fully renewable European power system. Renewable Energy, 63:467–476, March 2014.

[7] Sarah Becker, Rolando A. Rodríguez, Gorm B. Andresen, Stefan Schramm, and Martin Greiner. Transmission grid extensions during the build-up of a fully renewable pan-European electricity supply. Energy, 64:404–418, January 2014.

[8] Schaber, K., Steinke, F., and Hamacher, T. Transmission grid extensions for the integration of variable renewable energies in Europe: Who benefits where? Energy Policy, 43:123 – 135, 2012.

[9] Schaber, K., Steinke, F., Mühlich, P., and Hamacher, T. Parametric study of variable renewable energy integration in Europe: Advantages and costs of transmission grid extensions. Energy Policy, 42:498–508, 2012.

[10] Gorm Bruun Andresen, Anders Aspegren Søndergaard, and Martin Greiner. Validation of danish wind time series from a new global renewable energy atlas for energy system analysis. Energy, 2015.

[11] J. Widen. Correlations between large-scale solar and wind power in a future scenario for sweden. IEEE Transactions on Sustainable Energy, 2(2):177–184, 2011.

[12] RolandoA. Rodriguez, Magnus Dahl, Sarah Becker, and Martin Greiner. Localized vs. synchronized exports across a highly renewable pan-european transmission network. Energy, Sustainability and Society, 5(1), 2015.

[13] Magnus Dahl. Power-flow modeling in complex renewable electricity networks. Master's thesis, Aarhus University, 2015.

[14] Rolando A. Rodriguez, Sarah Becker, and Martin Greiner. Cost-optimal design of a simplified, highly renewable pan-european electricity system. Energy, 83:658 – 668, 2015.

[15] Rolando A. Rodriguez. Weather driven power transmission in a highly renewable European electricity network. PhD thesis, Aarhus University, 2014.

[16] Zuzana Dobrotkova, Al Goodrich, Miller Mackay, Cedric Philibert, Giorgio Simbolotti, and Professor XI Wenhua. Renewable energy technologies: Cost analysis series, solar photovoltaics. Technical Report 4/5, The International Renewable Energy Agency, 2012.

[17] Kost, C., Schlegl, T., Thomsen, J., Nold, S., and Mayer, J. Levelized cost of electricity: renewable energies. Technical report, Fraunhofer Institute for solar energy systems ISE, 2012. Online, retrieved October 2013.

[18] McKinsey. RoadMap 2050: A Practical Guide to a Prosperous, Low-Carbon Europe. Technical report, European Climate Foundation, 2010. Online, retrieved October 2013.

[19] W. Short, D. Packey, and T. Holt. A manual for the economic evalua- tion of energy efficiency and renewable energy technologies. Technical report, National Renewable Energy Laboratory, 1995.

[20] Rodriguez, R.A., Becker, S., Andresen, G., Heide, D., and Greiner, M. Transmission needs across a fully renewable European power system. Renewable Energy, 63:467–476, 2014.

[21] J. A. Nelder and R. Mead. A simplex method for function minimization. The Computer Journal, 7(4):308–313, 1965.

[22] S. Kirkpatrick, C. D. Gelatt, and M. P. Vecchi. Optimization by simulated annealing. Science, 220(4598):671–680, 1983.

[23] David E. Goldberg. Genetic Algorithms in Search, Optimization and Machine Learning. Addison-Wesley Longman Publishing Co., Inc., Boston, MA, USA, 1st edition, 1989.

[24] Xin-She Yang and Suash Deb. Cuckoo search via lévy flights. In NaBIC, pages 210–214. IEEE, 2009.

[25] Emil Haldrup Eriksen. Optimal heterogeneity in a highly renewable pan-european electricity system based on wind, solar, hydro and biomass resources. Master's thesis, Aarhus University, 2015.

[26] Stefan Bofinger, Lüder von Bremen, Kaspar Knoor, Katharina Lesch, Kurt Rohrig, Yves-Marie Saint-Drenan, and Markus Speckmann. Raum-zeitliche erzeugungsmuster von wind- und solarenergie in der ucte-region und deren einfluss auf elektrische transportnetze. Technical report, Institut für Solare Energieversorgungstechnik, 2008.

[27] G. Corbetta, I. Pineda, and J. Wilkes. Wind in power 2014 european statistics. Technical report, The European Wind Association, 2015.

[28] Vishal Shah, Jerimiah Booream-Phelps, and Susie Min. 2014 outlook: Let the second gold rush begin. Technical report, Deutsche Bank Markets Research, 2014.

Appendix I. Greedy Axial Search

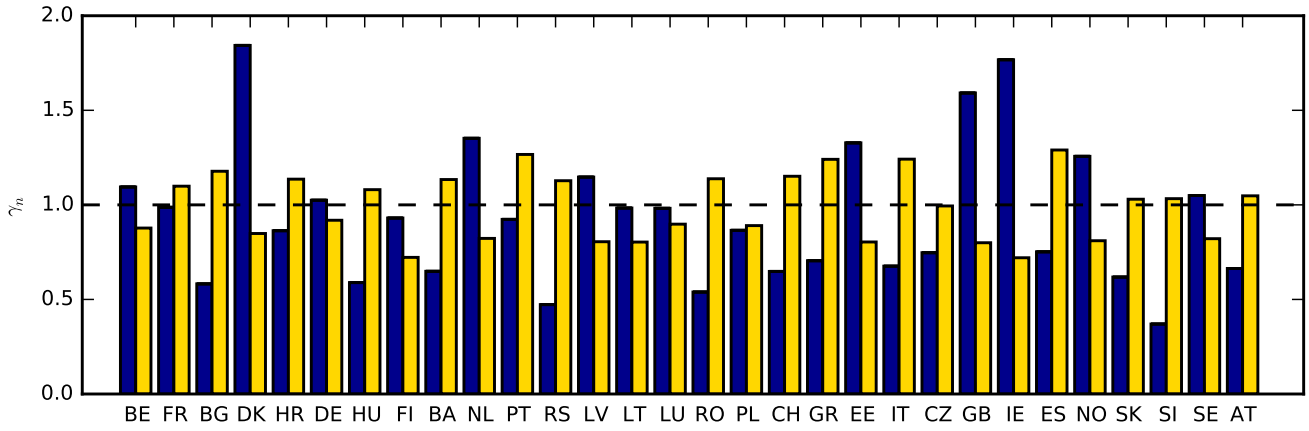

(a) Examples of β layouts for $\beta = 1$.

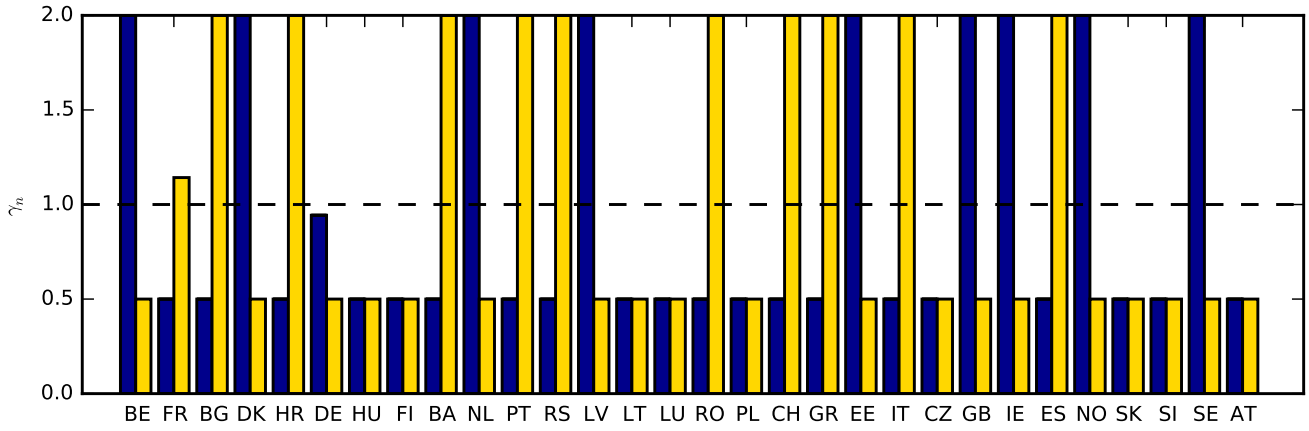

(b) Examples of CF layouts constrained by K = 2 .

Figure 2: Examples of heuristic layouts. In each sub figure, two sets of bars are shown corresponding to the $\alpha = 1$ and the $\alpha = 0$ layouts..

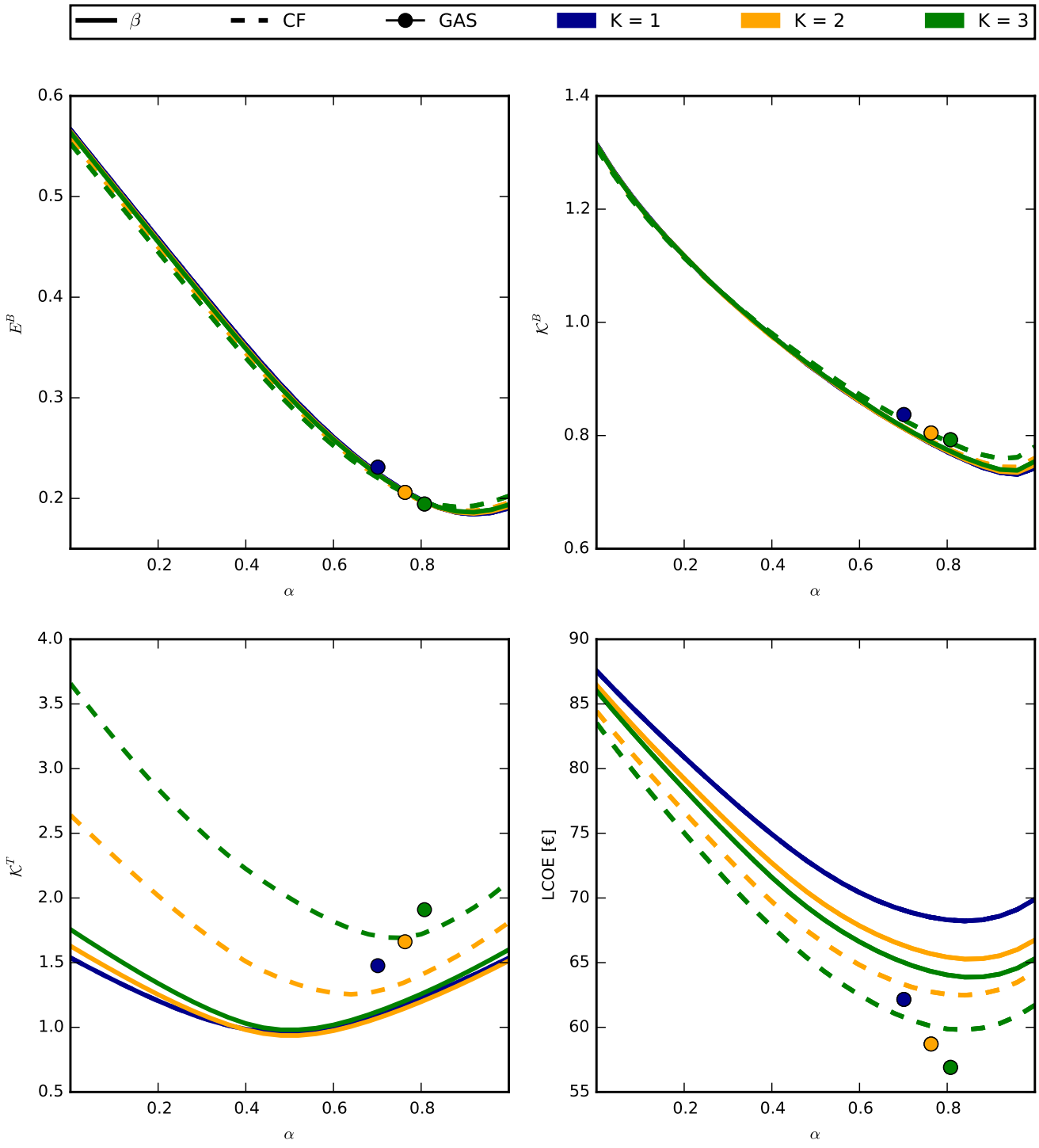

Figure 3: Overview of the key parameters and the associated LCOE as a function of α_{EU}. The β and CF layouts are shown as solid and dashed lines respectively. The GAS layouts are plotted as dots. Different constraints are shown: K = 1 (blue), 2 (yellow) and 3 (green).

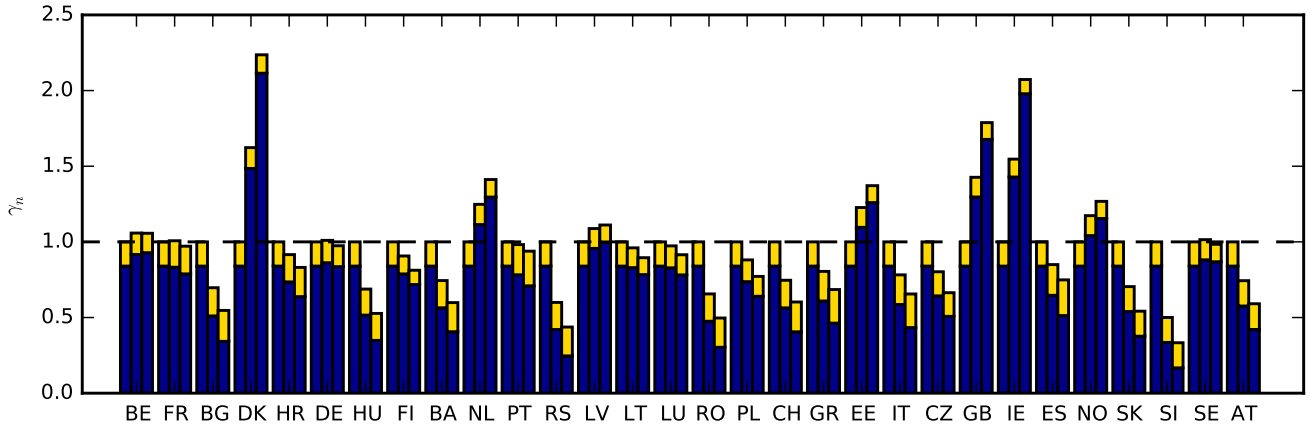

(a) Optimal β layouts (optimal mix at $\alpha = 0.84$).

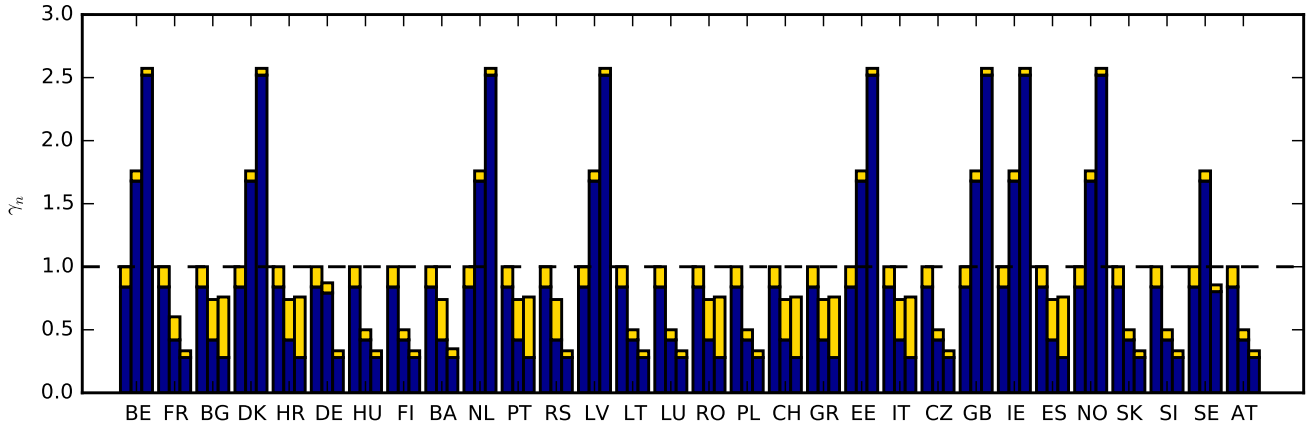

(b) Optimal CF layouts (optimal mix at $\alpha = 0.84$).

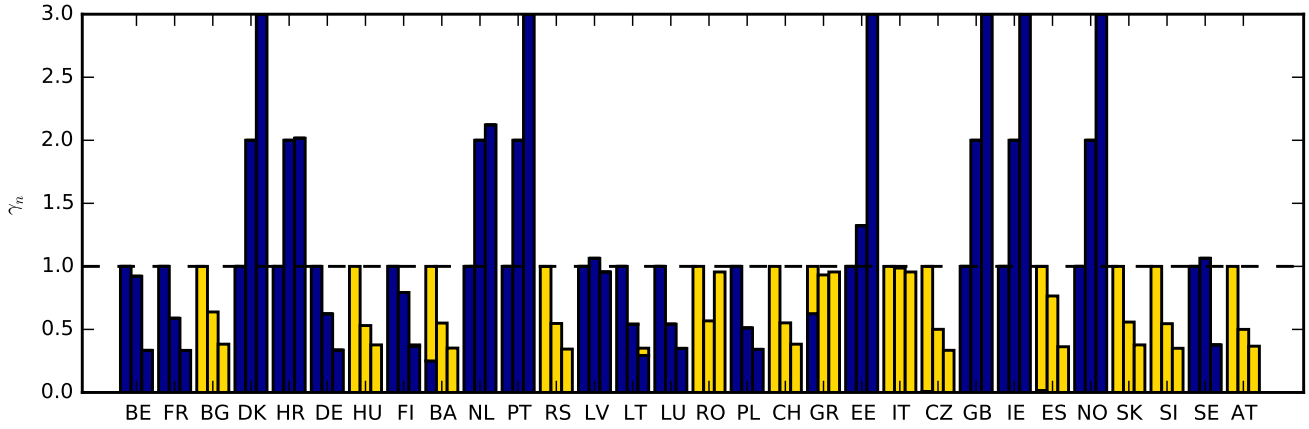

(c) GAS optimized layouts.

Figure 5: Optimal layouts. In each sub figure, three sets of bars corresponding to values of K = 1 (left), 2 (middle), and 3 (right) are shown.

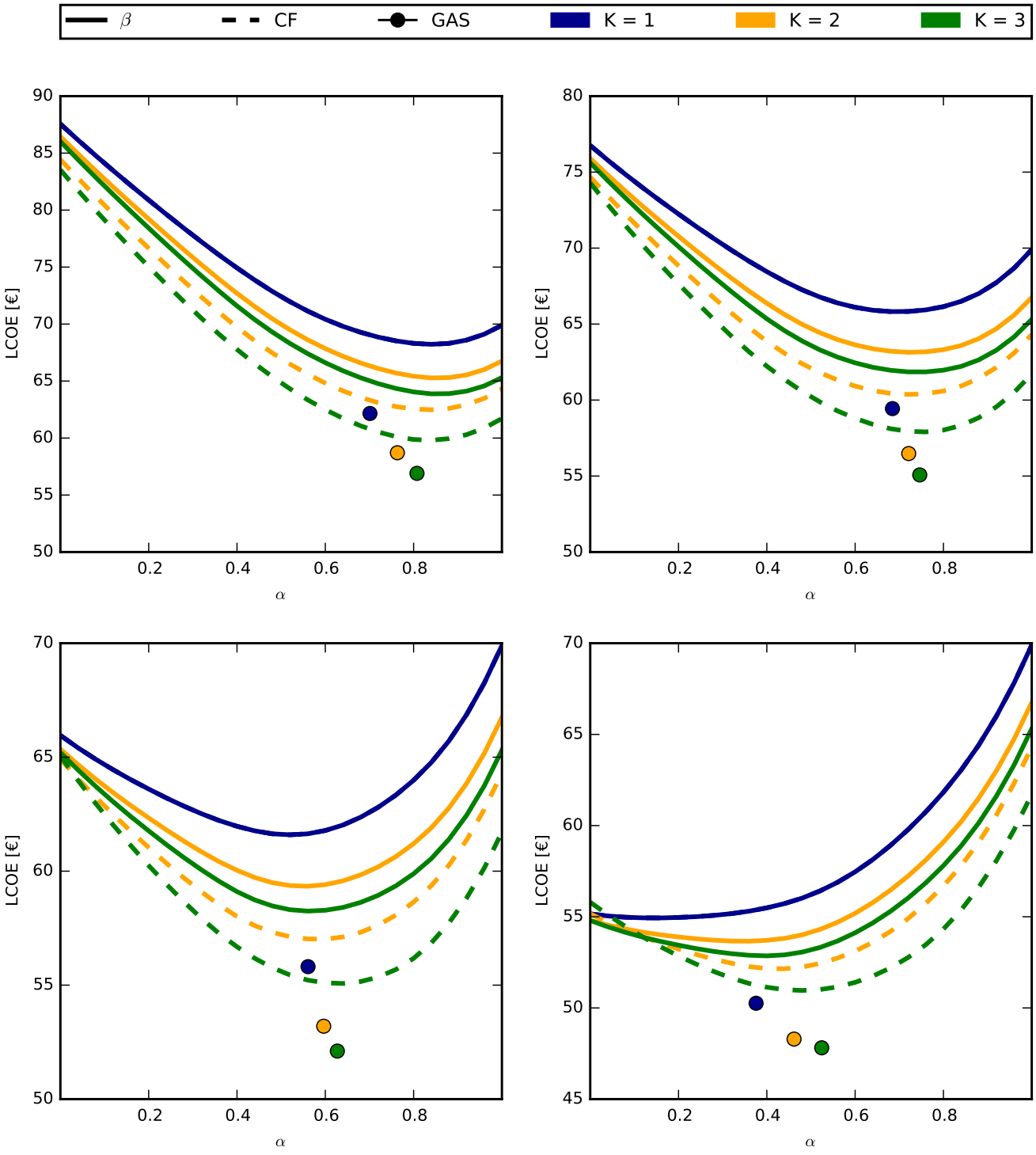

Figure 6: LCOE for different magnitudes of the solar cost reduction. Shown are cost reductions by 0% (top left), 25% (top right), 50% (bottom left) and 75% (bottom right).

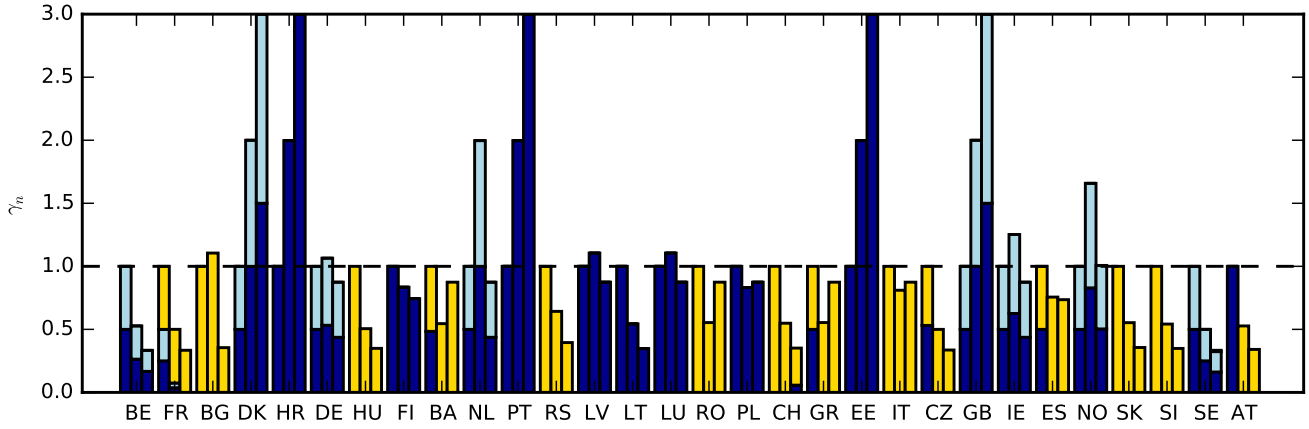

Figure 8: GAS optimised layouts constrained by K = 1 (left), 2 (middle) and 3 (right) for an offshore share of 50% for the North Sea contries.